Electronic Supplementary Material (ESI) for Dalton Transactions.
This journal is © The Royal Society of Chemistry 2020

Supporting Information

Synthesis and Characterization of the Mixed-Ligand Coordination Polymer $Cu_3Cl(N_4C\text{-}NO_2)_2$

Bradley Westwater, Hayleigh J. Lloyd, Inigo J. Victorica-Yrezabal, Angela Fong, Patrick McMaster, Martin Sloan, Brian M. Coaker, Colin R. Pulham, Peter Portius*

Email: p.portius@sheffield.ac.uk

Table of Contents

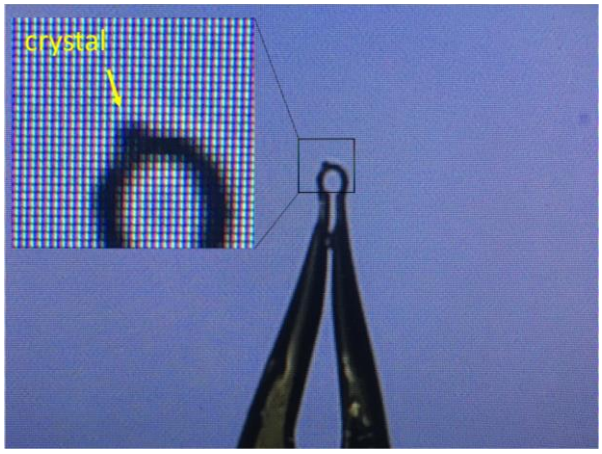

Figure S1. Photograph of a $Cu_3Cl(N_4C\text{-}NO_2)_2$ (**3**) crystal mounted on the goniometer nylon loop.

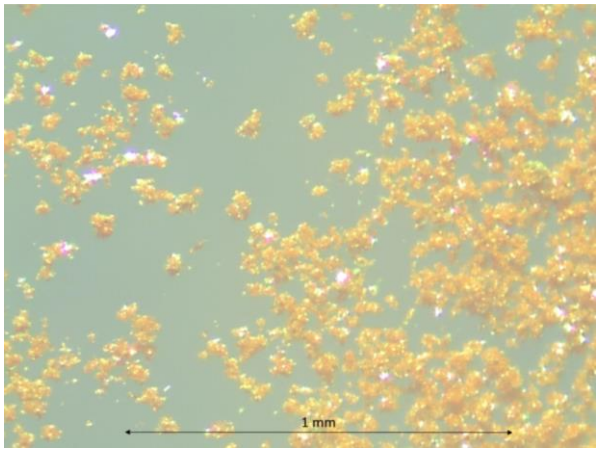

Figure S2. Microscope image of microcrystals of **3**, NB: back-lighting changes the apparent colour of the crystals.

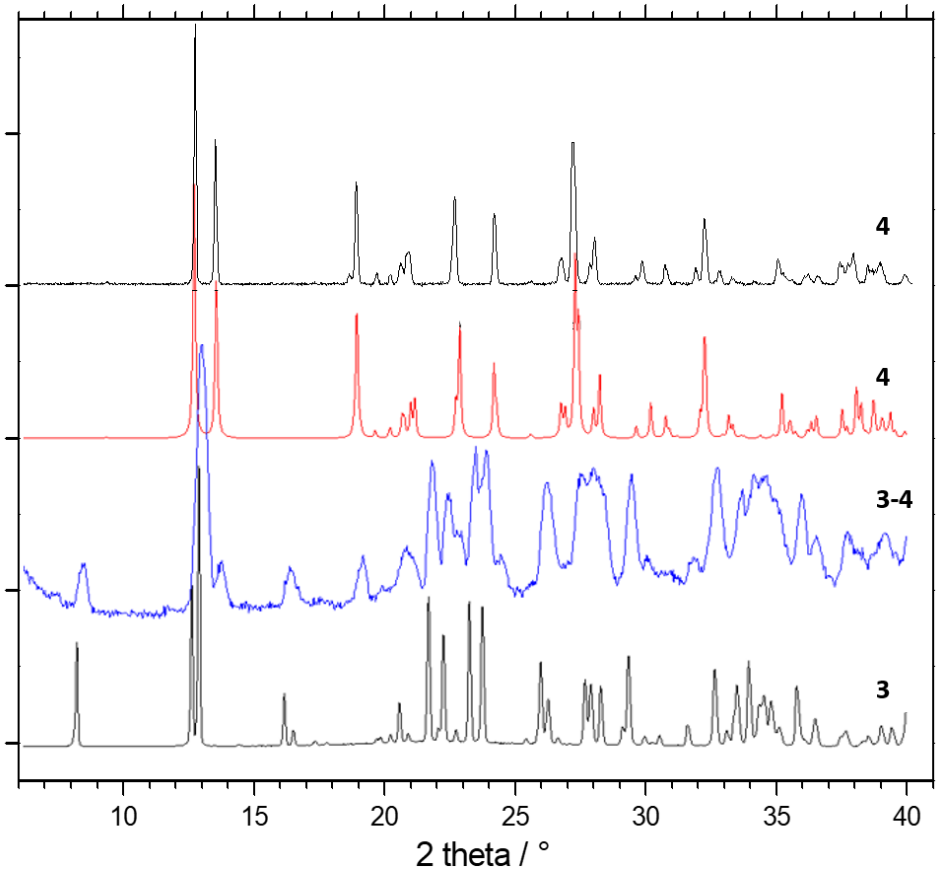

Figure S3. Powder diffractograms of pure **3** (bottom) and pure **4** (top, experimental —, predicted from single crystal data —) and of a mixture of **3** and **4** (—).

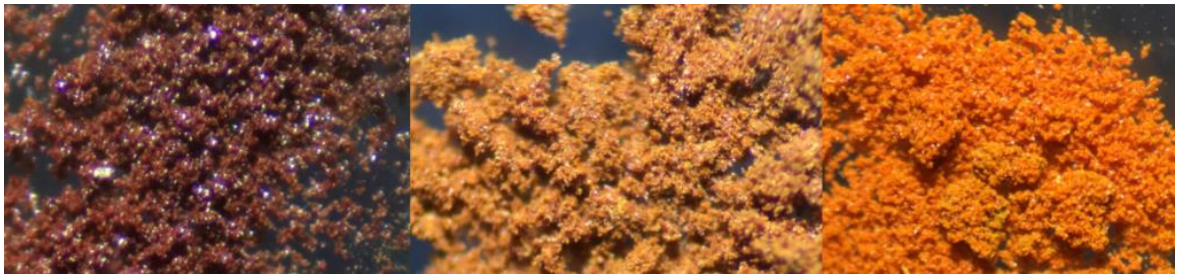

Figure S4. Images of microcrystalline powders of **3** (left), a mixture of **3** and **4** (middle), and **4** (right). All images were taken at the same degree of magnification.

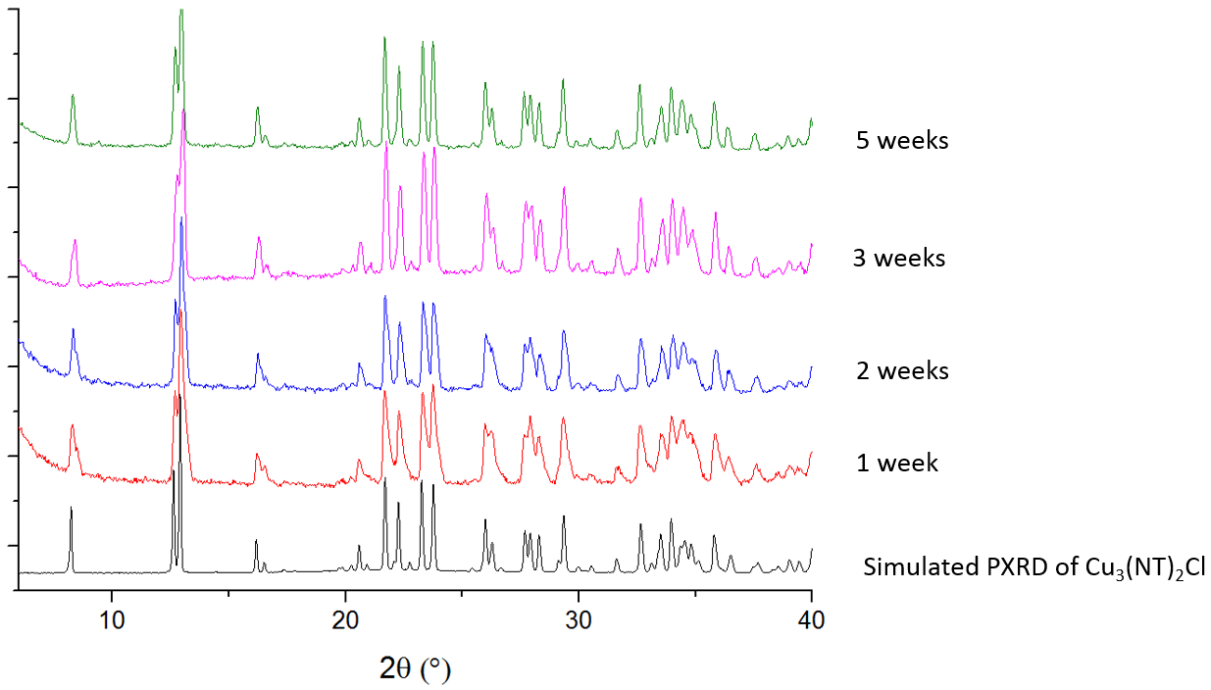

Figure S5a. PXRD of compound **3** recorded after exposure to air for the duration of time as indicated.

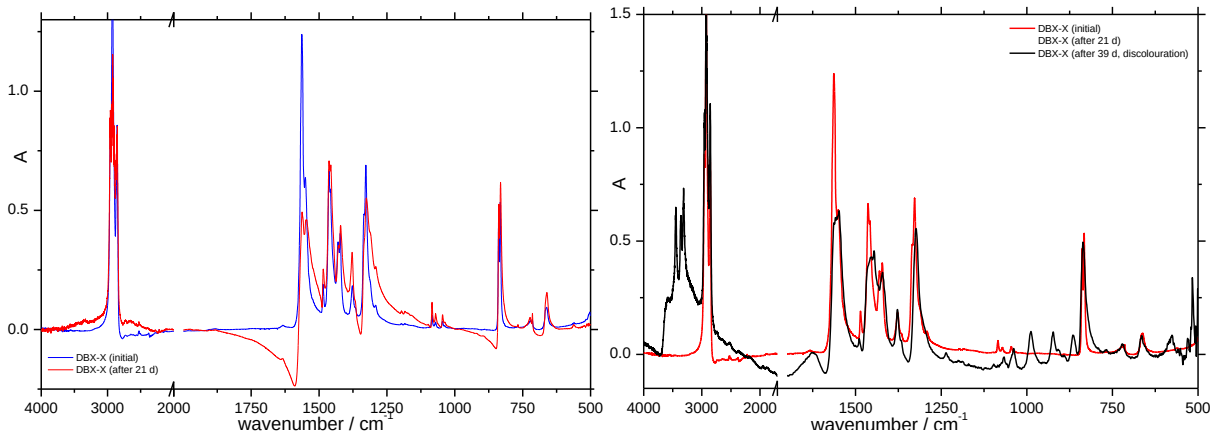

Figure S5b. FTIR spectra of compound **3** recorded after exposure to air (left) and water (right) for the durations of time as indicated.

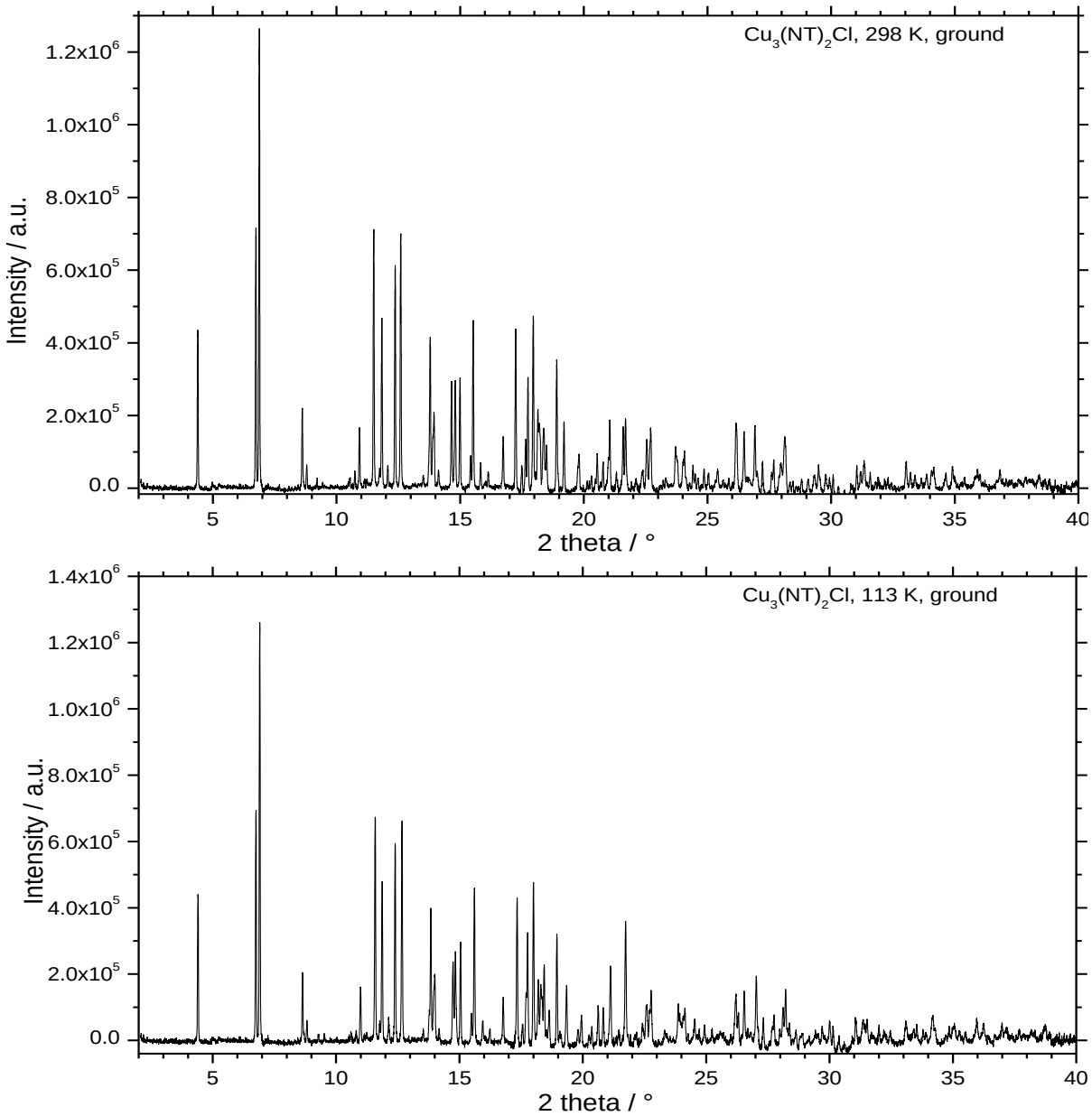

Figure S5c. Powder diffractograms of compound **3** (capillary tube, λ = 0.82471(1) Å, at 113 K (bottom) and 298 K (top)).

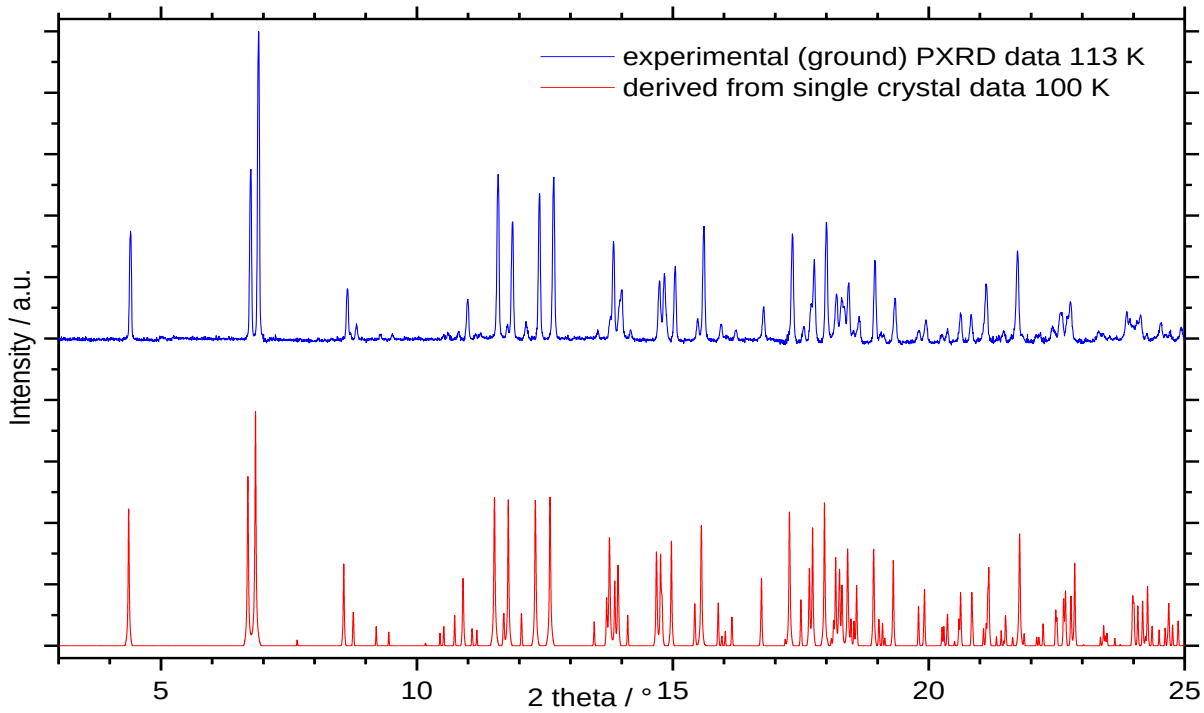

Figure S6. Powder diffractograms (shown between 3° and 25° 2θ) for compound **3** obtained by powder diffractometry (capillary tube, λ = 0.82471(1) Å, at 113 K) (top), and by prediction from single crystal XRD data obtained at 100 K (bottom), for the same the same wavelength.

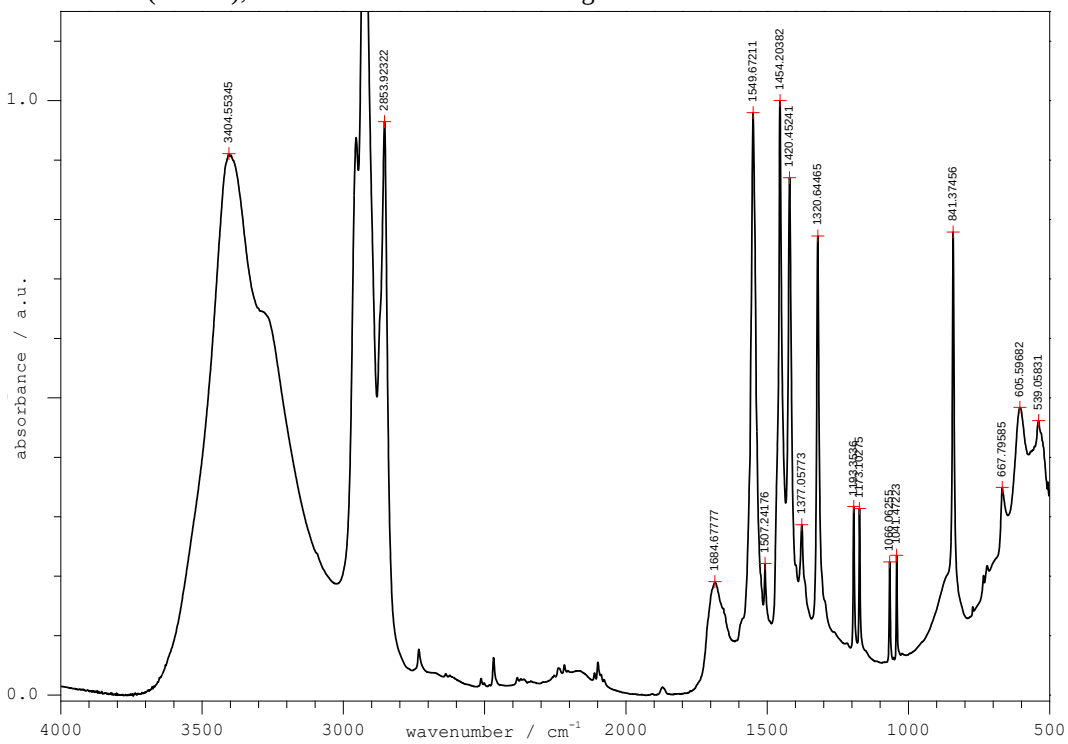

Figure S7. Infrared spectrum of NaNT.2$H_2$0 (**1**).

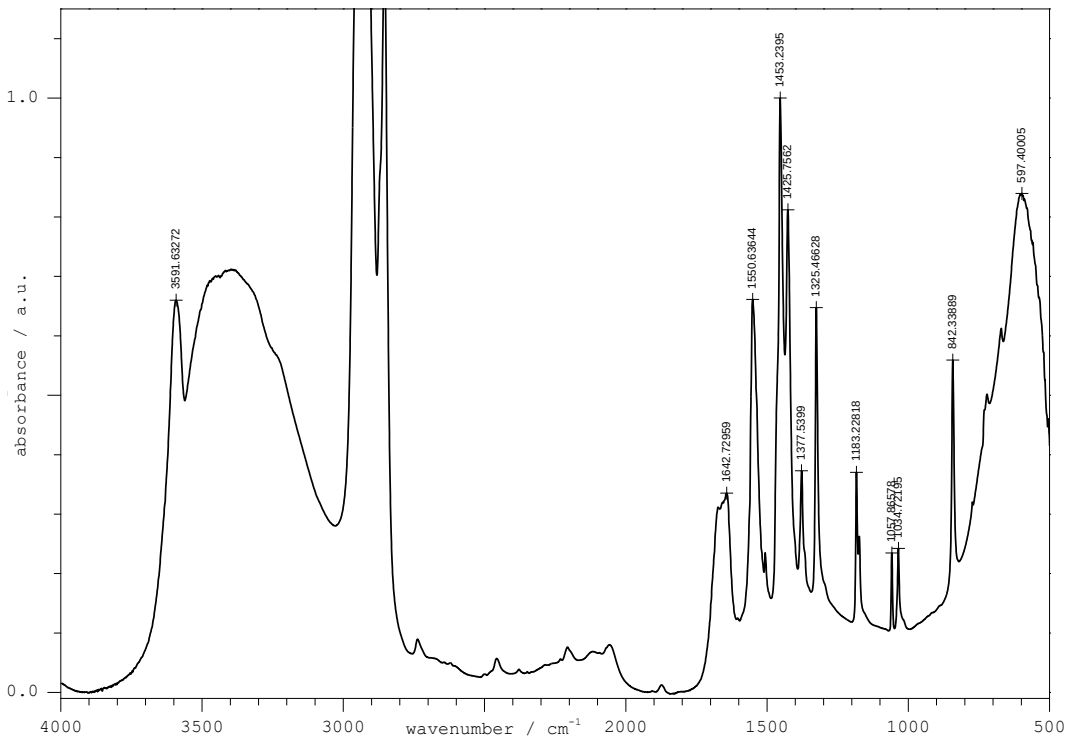

Figure S8. Infrared spectrum of NaNT.4$H_2$0 (**2**).

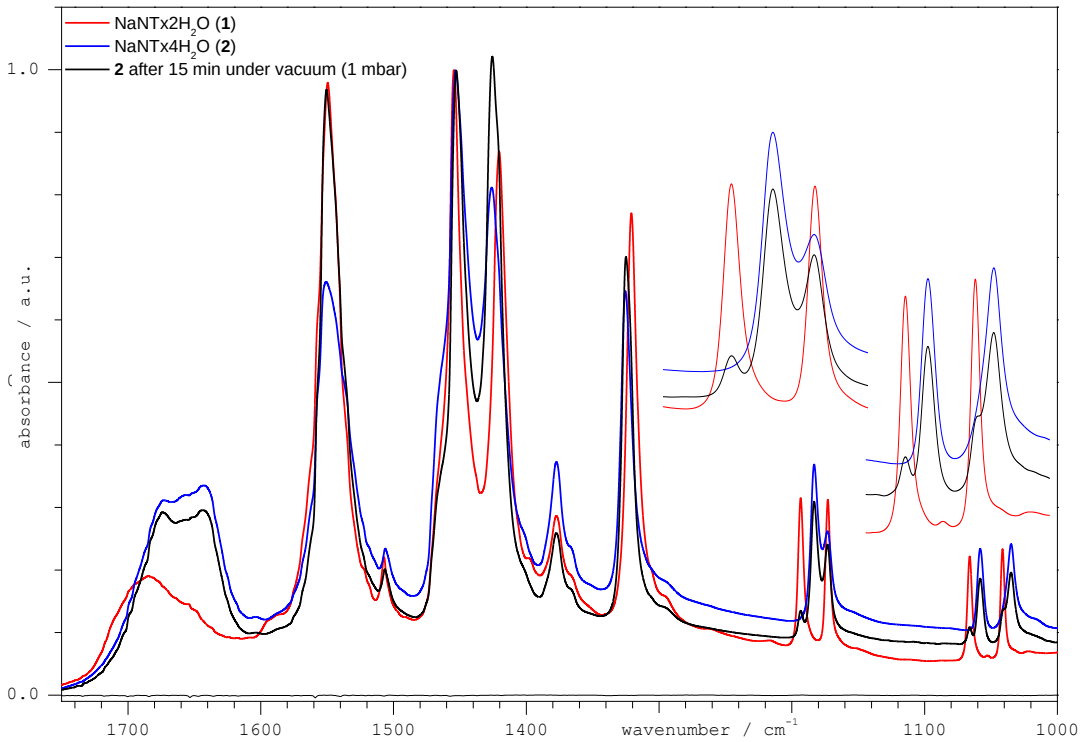

Figure S9. Infrared spectra of **1** and **2** 1720-1000 cm^{-1}, showing the effect of dehydration on **2** under vacuum. The diagnostic region 1200-1000 cm^{-1} shown as enlarged insets; mulling agent peaks (liquid paraffin) at 1463 cm^{-1} (sholder) and 1377 cm^{-1}.

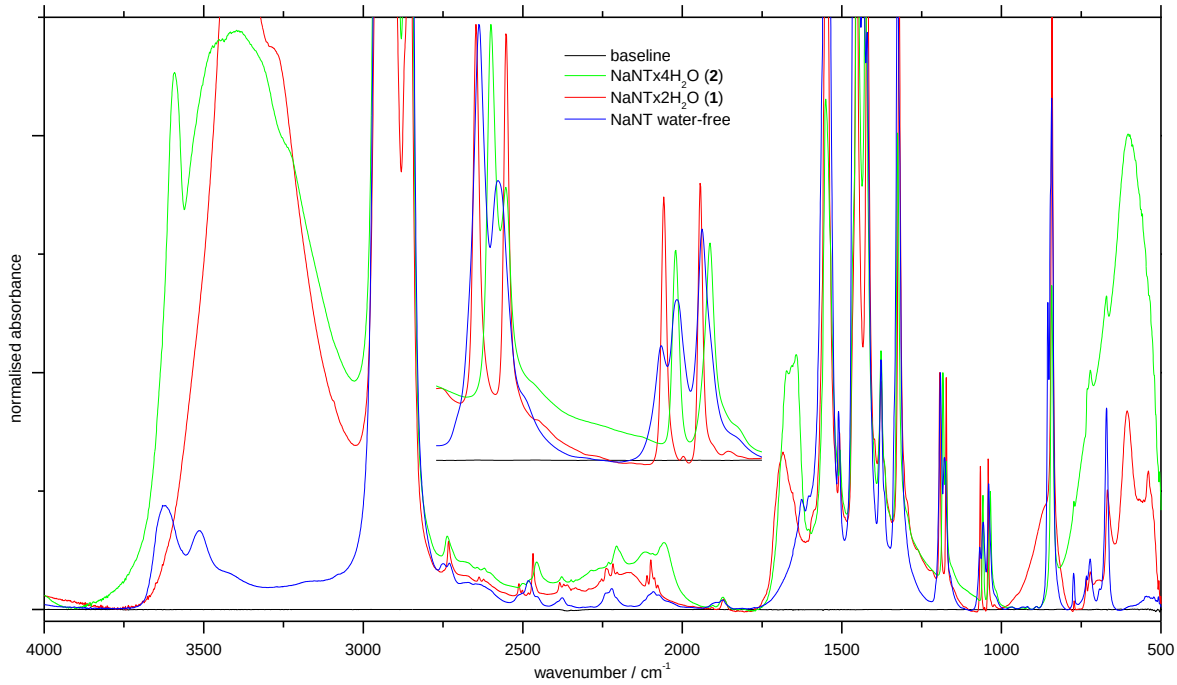

Figure S10. Infrared spectra of NaNT.4H_2O (**1**), NaNT.2H_2O (**2**) and water-free NaNT. The diagnostic region 1200-1000 cm^{-1} shown as enlarged insets; mulling agent peaks (liquid paraffin) at 2954-2853, 1463, 1377 and 721 cm^{-1}.

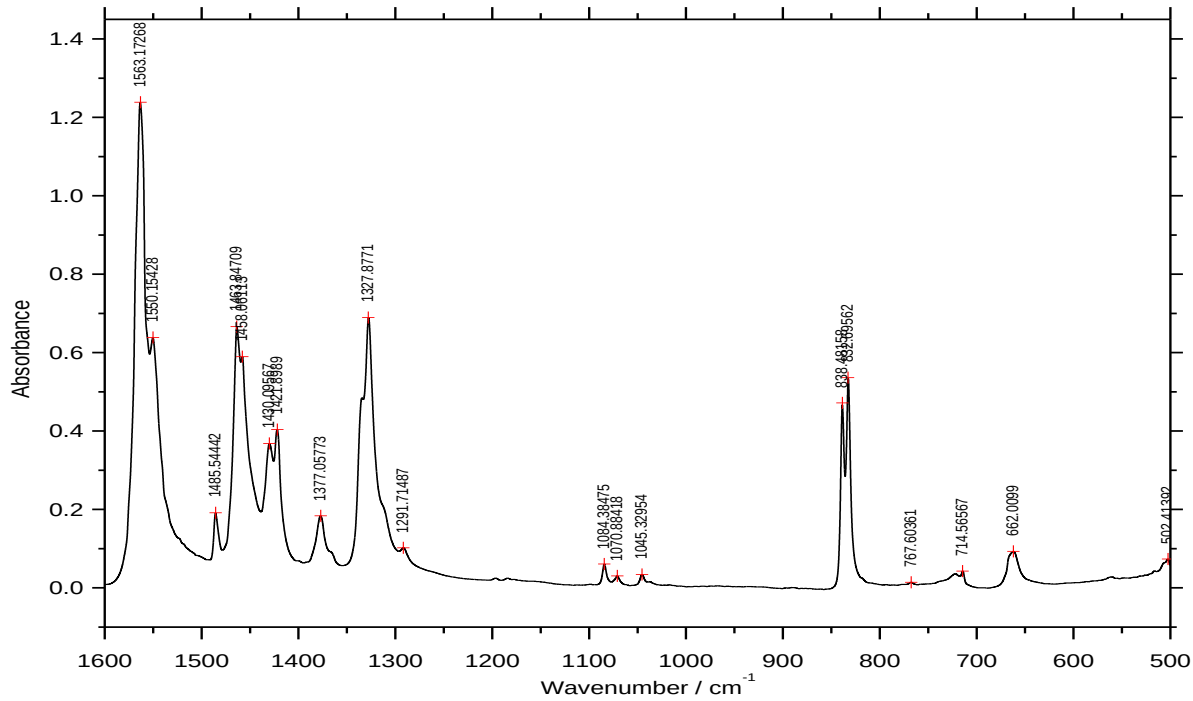

Figure S11. FTIR spectrum (transmission, mull) of **3**, expanded range 1600 to 500 cm^{-1} shown.

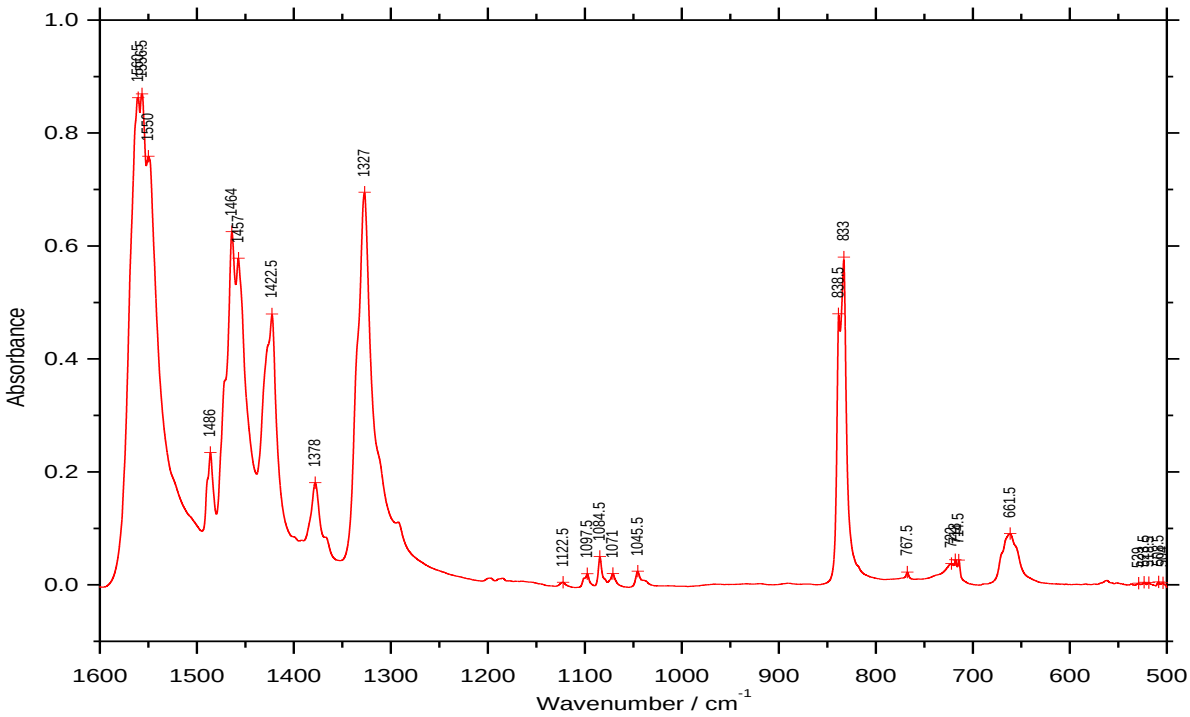

Figure S12. FTIR spectrum (transmission, mull) of a **3** / **4** mixture, expanded range 1600 to 500 cm^{-1} shown.

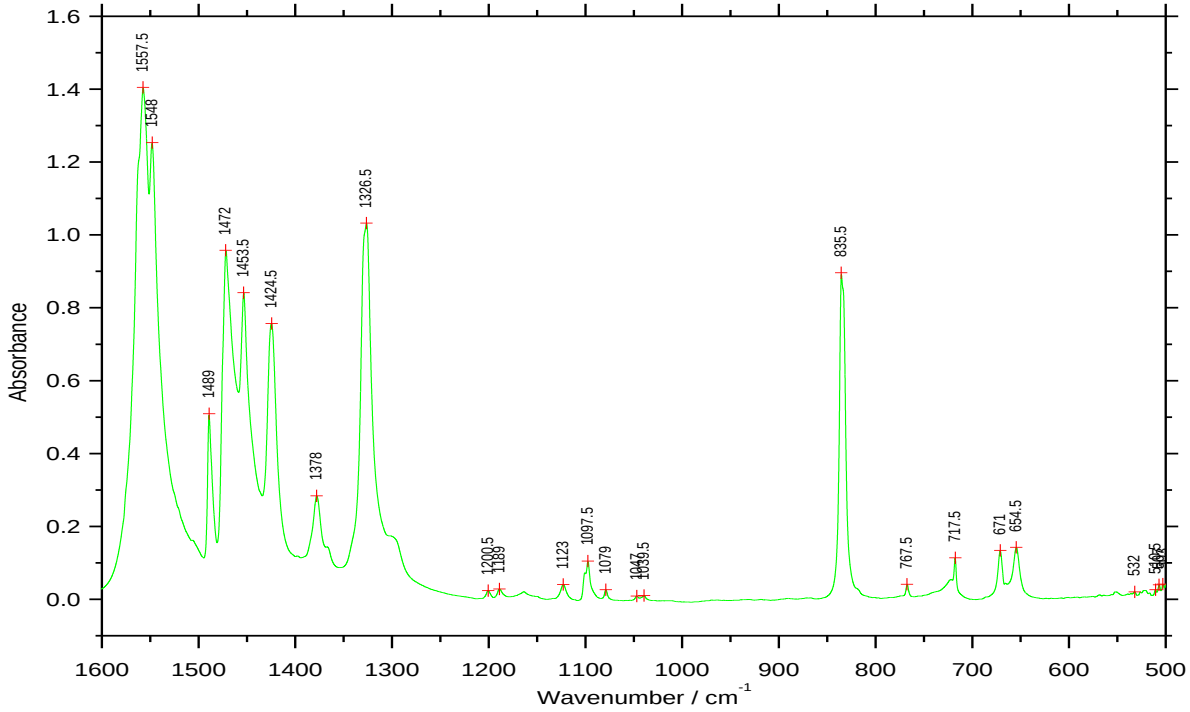

Figure S13. FTIR spectrum (transmission, mull) of **4**, expanded range 1600 to 500 cm^{-1} shown.

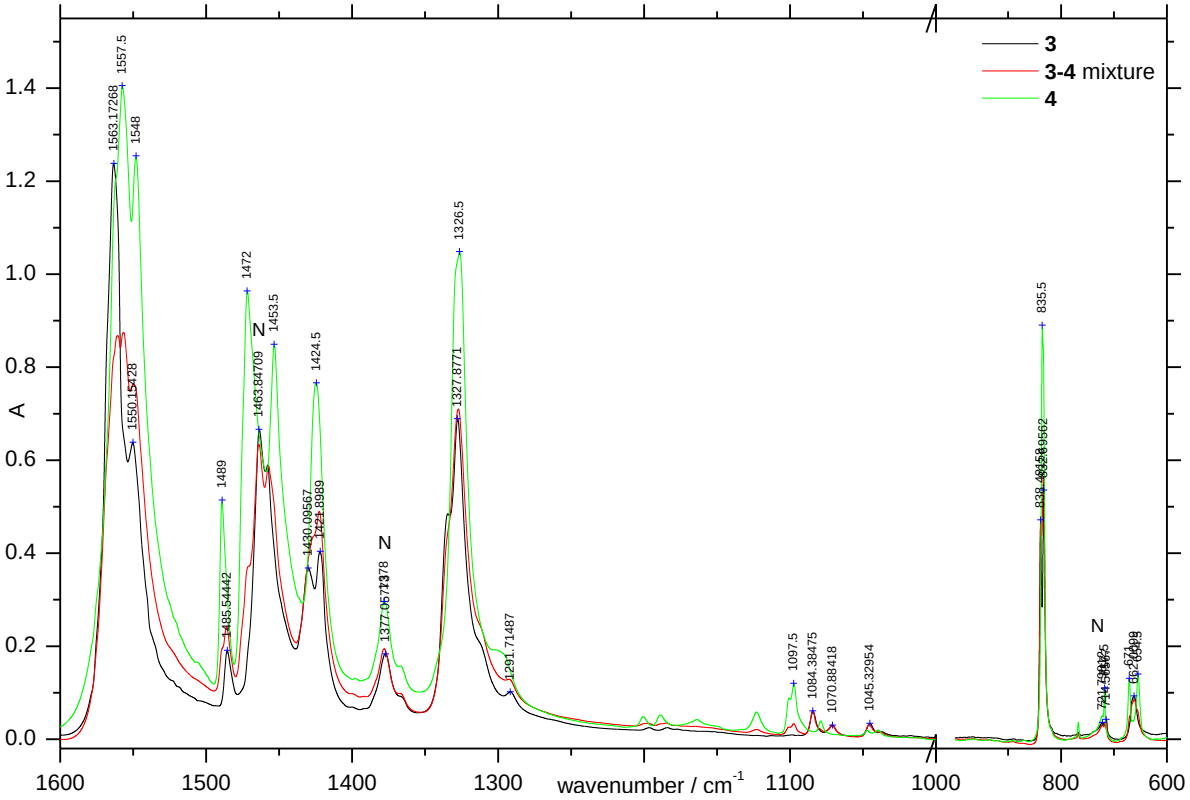

Figure S14. Infrared spectra of **3** and **4** in the region 1600-600 cm^{-1}; mulling agent peaks are labelled by "N"; note the scale change at 1000 cm^{-1}.

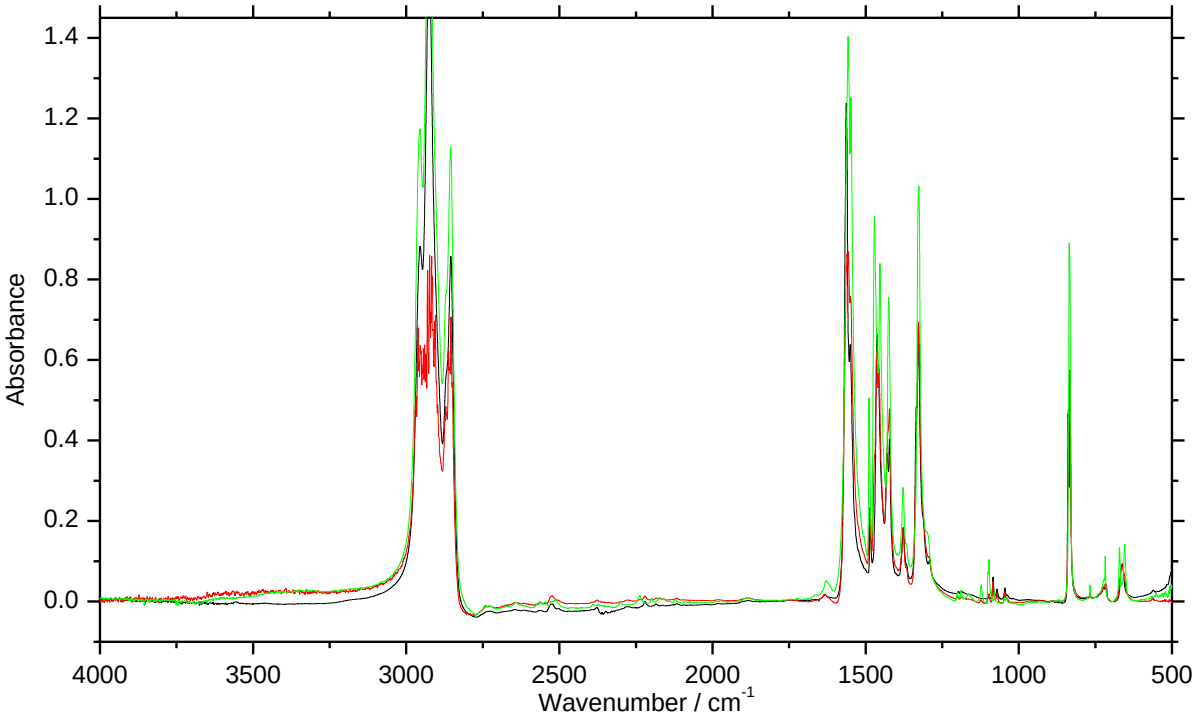

Figure S15. Infrared spectra of Fig. S14 in the range 4000-500 cm^{-1}.

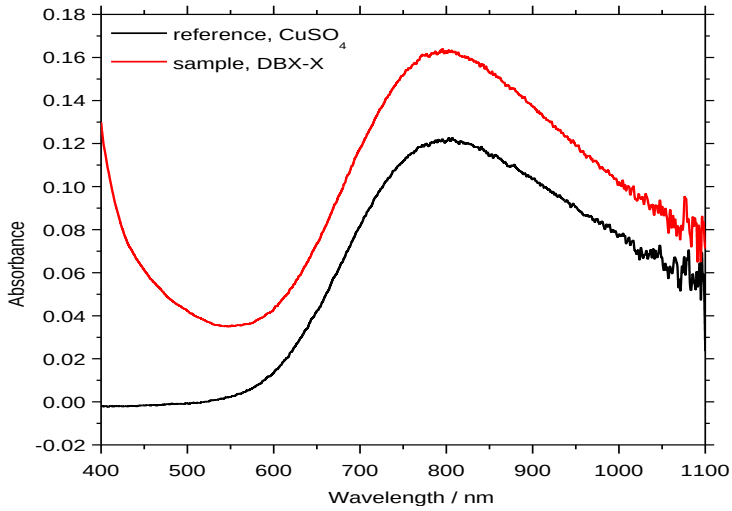

Figure S16. UV/vis absorption spectra of $CuSO_4$ and compound **3** after digestion in aqueous nitric acid (65%). Both spectra were recorded in 65% aqueous nitric acid. Both peak maxima are at 801 nm.

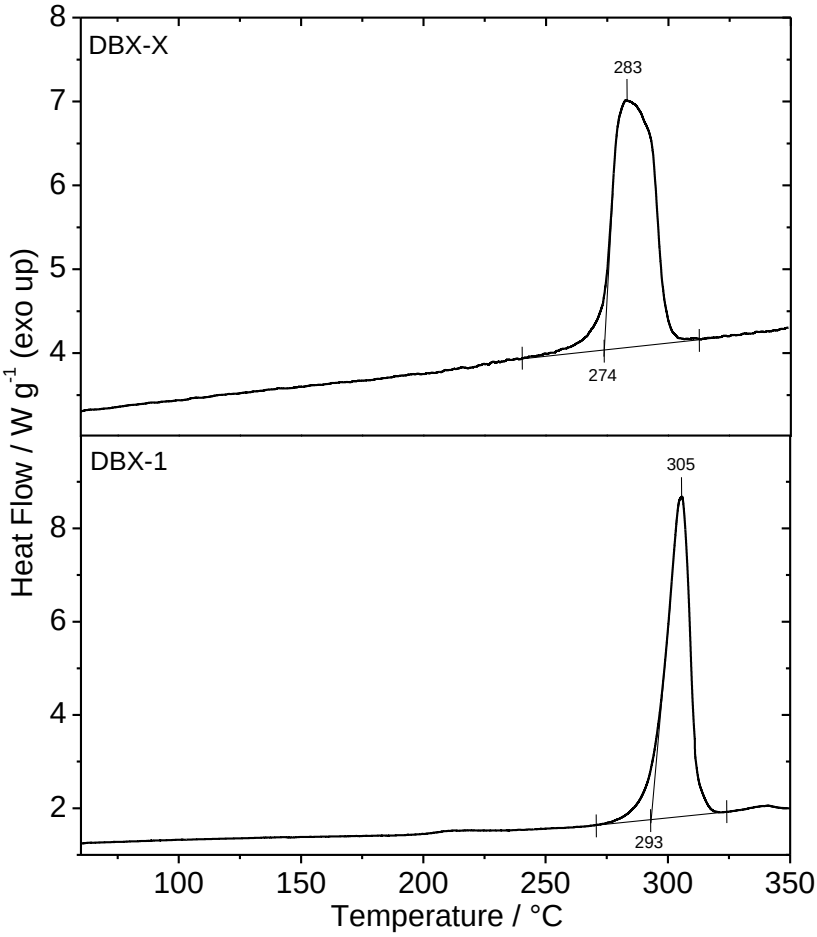

Figure S17. DSC calorigrams compounds **3** (top) and **4** (bottom), scan rate 3 K min^{-1}.

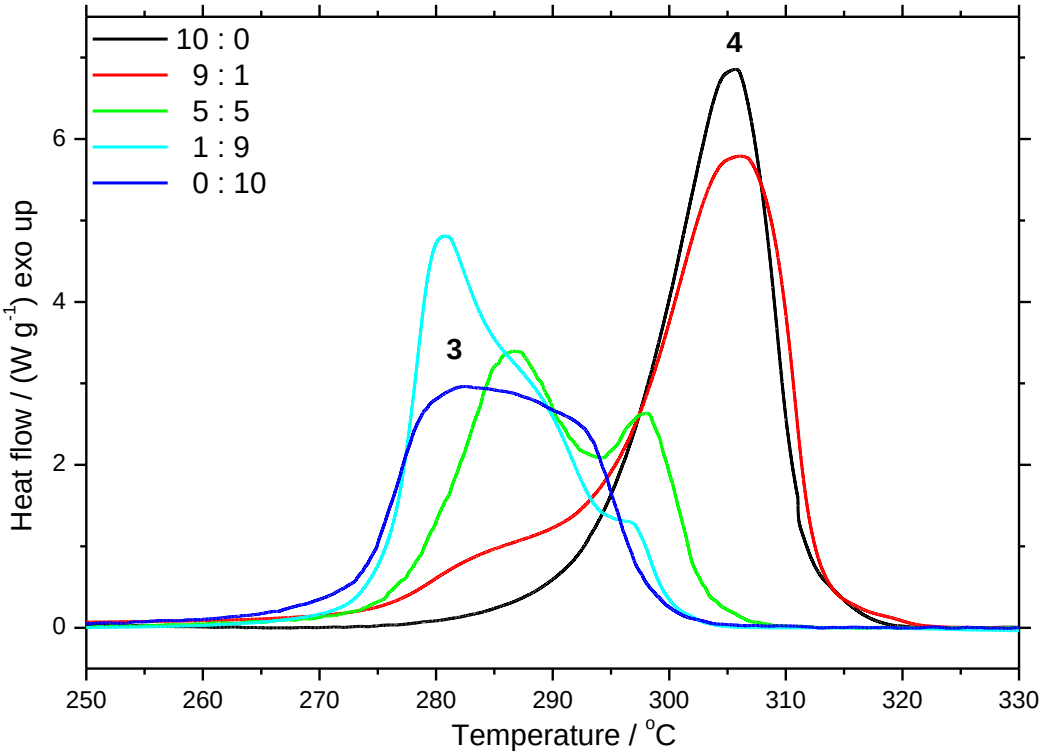

Figure S18. DSC calorigrams compounds **3** (top) and **4** (bottom), scan rate 3 K min^{-1}.

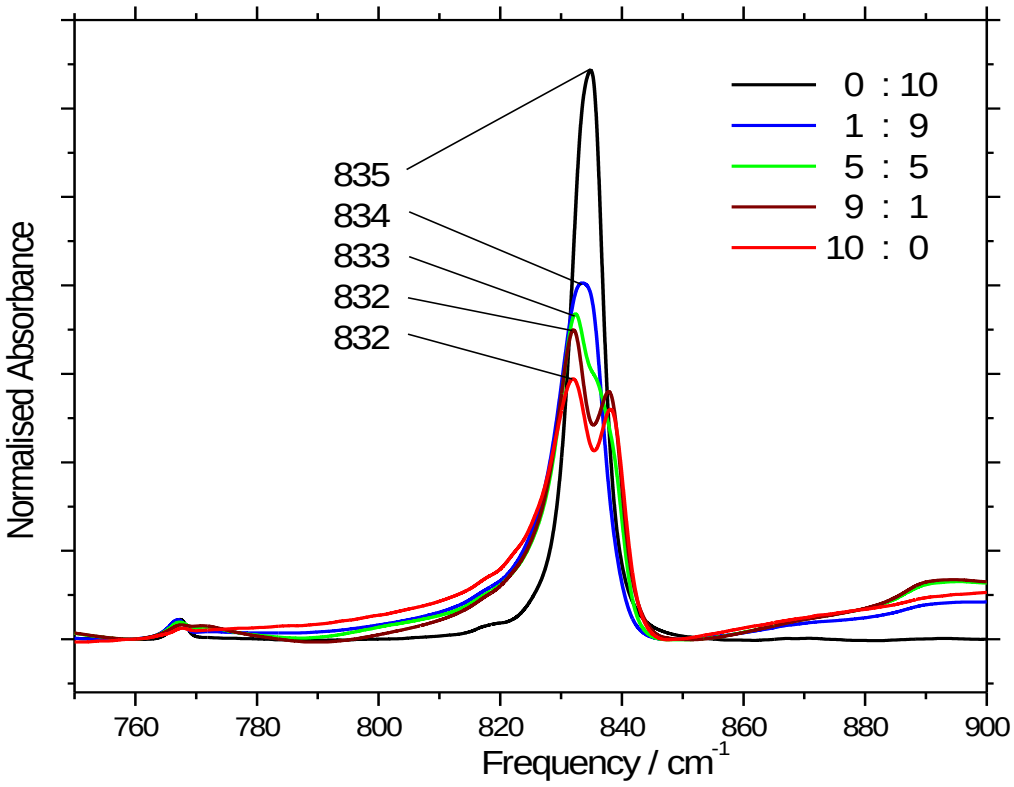

Figure S19. Baseline-corrected section of IR spectra (transmission in nujol) between 750 and 900 cm^{-1} **4** (black), **3** (red) on left. Spectra are normalised by the absorption integrated between 786-848 cm^{-1}.

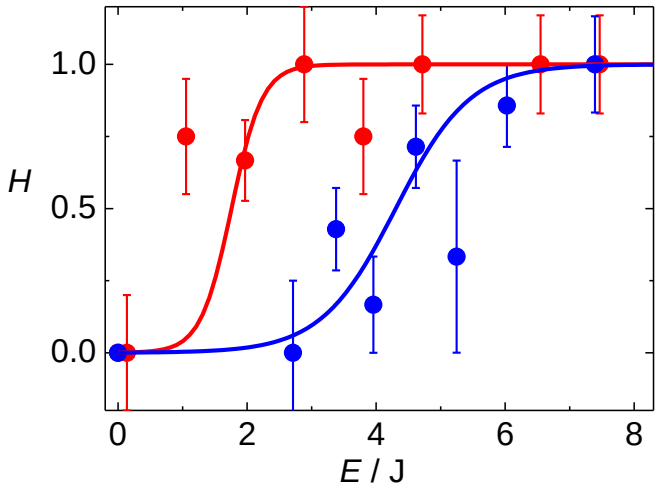

Figure S20. Histogram showing the probability of initiation of samples of $Cu_3Cl(O_2N\text{-}CN_4)_2$ (●) and $Cu(O_2N\text{-}CN_4)$ (●). The E_{50} values and margins of error were determined by curve-fitting using the sigmoidal function $H = a / [1 - e^{-k(E - E50)}]$.

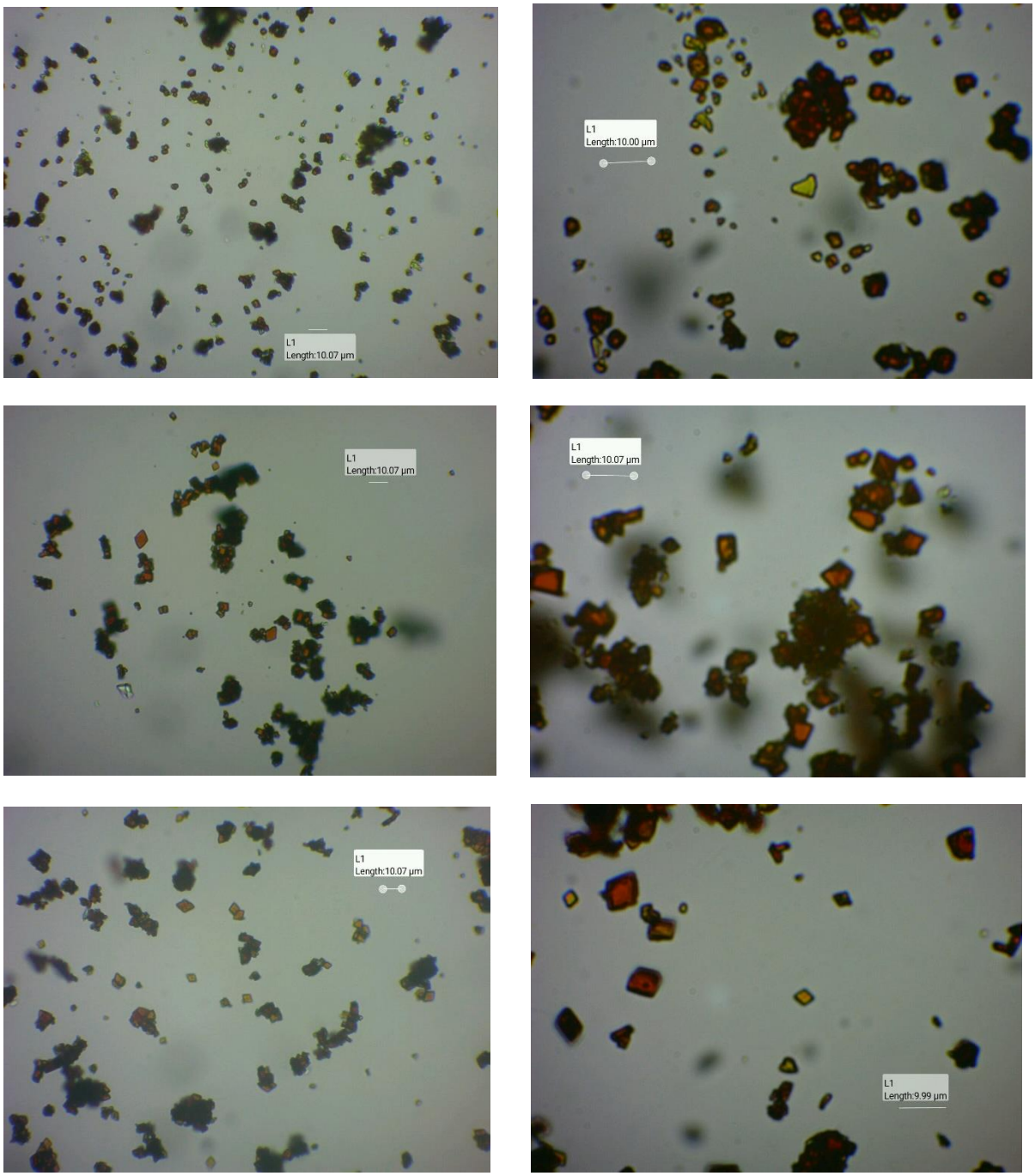

Figure S21. Microscope images of three batches of $Cu_3Cl(O_2N\text{-}CN_4)_2$ (top [$ZnBr_2$-seeded], middle, bottom [not intentionally seeded]) at 40x (left column) and 100x (right column) magnification. The length scales are shown by horizontal white lines.

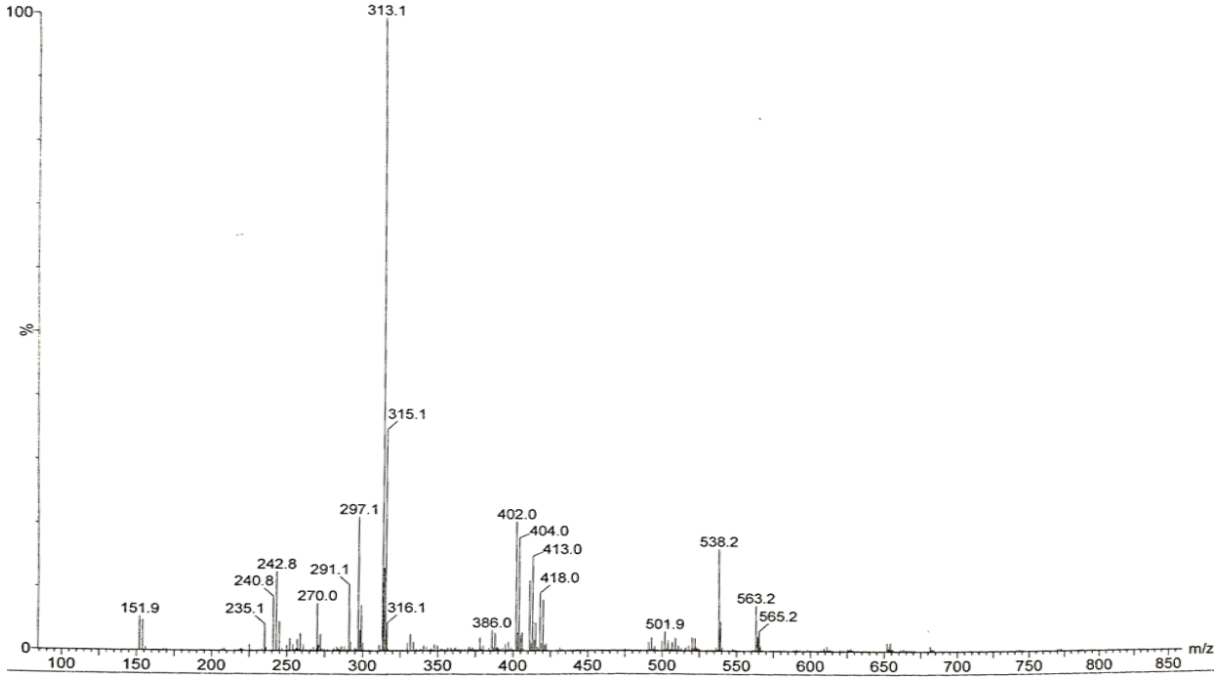

Figure S22. TOF LD(+) MS spectrum.
Note: the peak at m/z = 538 is likely to be caused by DCTP.

Table S1. Preparative conditions for the reduction of $CuCl_2$ in the presence of NaNT for trials numbered in chronological order (No), yields given in %**.**

No	Conditions	Reagent 1	*c*	*v*	Reagent 2	*c*	*v*	Reagent 3	*c*	*v*	Product	Yield
1	vessel and stir bar rinsed with water and mechanically cleaned with cellulose paper	$CuCl_2$	1.02	1.00	$NaNT(H_2O)_2$ batch 1	0.46	0.93	Na H-Asc	1.00	0.50	amorphous air sensitive solid	-
2	vessel and stir bar rinsed with water and mechanically cleaned with cellulose paper	$CuCl_2(H_2O)_2$	1.00	1.00	$NaNT(H_2O)_4$ batch 1	0.47	0.82	Na H-Asc	1.00	0.50	$Cu_3Cl(N_4CNO_2)_2$	86
3	vessel and stir bar rinsed with water and mechanically cleaned with cellulose paper	$CuCl_2(H_2O)_2$	0.18	1.00	$NaNT(H_2O)_4$ batch 1	0.66	1.17	Na H-Asc	1.00	0.50	$Cu_3Cl(N_4CNO_2)_2$	86
4	vessel and stir bar rinsed with water and mechanically cleaned with cellulose paper; only deionised water used that was purified further by distillation	$CuCl_2$	0.15	1.00	$NaNT(H_2O)_4$ batch 1	0.57	1.00	Na H-Asc	0.99	0.50	$Cu_3Cl(N_4CNO_2)_2$	83
5	vessel and stir bar rinsed with water and mechanically cleaned with cellulose paper	$CuCl_2$	0.15	1.00	$NaNT(H_2O)_4$ batch 1	0.46	0.94	Na H-Asc	1.00	1.00	Amorphous	-
6	vessel and stir bar rinsed with water and mechanically cleaned with cellulose paper	$CuCl_2$	0.14	1.00	$NaNT(H_2O)_4$ batch 1	0.46	1.00	Na H-Asc	0.97	0.50	$Cu_3Cl(N_4CNO_2)_2$	67
7	vessel and stir bar rinsed with water and mechanically cleaned with cellulose paper; only deionised water used that was purified further by distillation	$CuCl_2$	0.15	1.00	$NaNT(H_2O)_4$ batch 1	0.57	1.00	Na H-Asc	0.99	0.50	$Cu_3Cl(N_4CNO_2)_2$ / $CuCN_4NO_2$	73-86
8	vessel and stir bar rinsed with water and mechanically cleaned with cellulose paper	$CuCl_2$	0.15	1.00	$NaNT(H_2O)_4$ batch 1	0.45	1.00	Na H-Asc	0.50	0.50	$CuCN_4NO_2$	72
9	vessel and stir bar rinsed with water and mechanically cleaned with cellulose paper	$CuCl_2$	0.15	1.00	$NaNT(H_2O)_4$ batch 1	0.46	1.00	Na H-Asc	0.49	0.50	$CuCN_4NO_2$	71
10	vessel and stir bar rinsed with water and mechanically cleaned with cellulose paper	$CuCl_2$	0.15	1.00	$NaNT(H_2O)_4$ batch 1	0.47	1.00	Na H-Asc	1.00	0.50	$CuCN_4NO_2$	71
11	vessel treated with 65% aqueous HNO_3 and neutralised with deionised water	$CuCl_2$	0.15	1.00	$NaNT(H_2O)_4$ batch 2	0.46	1.00	Na H-Asc	0.98	0.50	amorphous solid	-

12	vessel and stir bar rinsed with water and mechanically cleaned with cellulose paper	CuCl2	0.15	1.00	$NaNT(H_2O)_2$ batch 2	0.47	1.00	Na H-Asc	0.99	0.50	amorphous solid	-
13	beaker treated with 65% aqueous HNO_3 and neutralised with deionised water; seeded with 10 – 15 mg $Cu(N_4CNO_2)$	$CuCl_2$	0.15	1.00	$NaNT(H_2O)_4$ batch 2	0.46	1.00	Na H-Asc	0.98	0.50	CuN_4CNO_2	65
14	beaker treated with 65% aqueous HNO_3 and neutralised with deionised water; seeded with 10 – 15 mg $Cu_3Cl(N_4CNO_2)_2$	$CuCl_2$	0.15	1.00	$NaNT(H_2O)_4$ batch 2	0.46	1.01	Na H-Asc	0.99	0.50	CuN_4CNO_2	69
15	beaker treated with 65% aqueous HNO_3 and neutralised with deionised water; seeded with 10 – 15 mg $Cu_3Cl(N_4CNO2)_2$	$CuCl_2$	0.15	1.00	$NaNT(H_2O)_4$ batch 2	0.46	1.01	Na H-Asc	0.98	0.50	$Cu_3Cl(N_4CNO_2)_2$ / $CuCN_4NO_2$	67-79
16	beaker only rinsed with deionized water	$CuCl_2$	0.15	1.00	$NaNT(H_2O)_4$ batch 2	0.47	1.00	Na H-Asc	0.98	0.50	$CuCN_4NO_2$	61
17	seeded with 10 to 15 mg $Cu(N_4CNO_2)$	$CuCl_2$	0.15	1.00	$NaNT(H_2O)_2$ batch 3	0.56	1.20	Na H-Asc	0.99	0.50	amorphous air sensitive solid	-
18	vessel and stir bar rinsed with water and mechanically cleaned with cellulose paper	$CuCl_2$	0.14	1.00	$NaNT(H_2O)_4$ batch 3	0.56	1.20	Na H-Asc	0.88	0.50	CuN_4CNO_2	72
19	vessel and stir bar rinsed with water and mechanically cleaned with cellulose paper	$CuCl_2$	0.15	1.00	$NaNT(H_2O)_4$ batch 4	0.31	0.67	Na H-Asc	1.00	0.50	amorphous air sensitive solid	-
20	seeded with 10 to 15 mg $Cu_3Cl(N_4CNO_2)_2$	$CuCl_2$	0.15	1.00	$NaNT(H_2O)_4$ batch 4	0.31	0.67	Na H-Asc	0.99	0.50	amorphous solid; red material deposited on vessel walls	-
21	beaker only rinsed with deionized water	$CuCl_2$	0.15	1.00	$NaNT(H_2O)_4$ batch 4	0.47	1.00	Na H-Asc	0.98	0.50	amorphous solid; 64 mg dark red material deposited on vessel walls	15

NB: *c* and *v* refer to reagent concentration (mol dm^{-3}) and the stoichiometric coefficient, respectively.

***Table S2*.** Key energetic materials parameters of compounds **1**-**4** and **LA**.

	$Na(N_4C\text{-}NO_2)\cdot 2H_2O$ (**1**)	$Na(N_4C\text{-}NO_2)\cdot 4H_2O$ (**2**)	$Cu_3Cl(N_4C\text{-}NO_2)_2$ (**3**)	$Cu(N_4C\text{-}NO_2)$ (**4**)	α-$Pb(N_3)_2$ (**LA**)
T_{dec}^{on} / °C	-	-	274 [a]	293 [a]	313 [b]
ΔH_{exo} / (kJ mol^{-1})	-	-	546 [c]	294 [c]	443 [d]
ΔH_{exo} / (kJ g^{-1})	-	-	1.201 [a]	1.653 [a]	1.52 [e]
ΔH_{exo} / (kJ cm^{-3})	2.9 [f,g]	2.4 [f,g]	3.5 [g]	4.3 [g]	7.2 [g]
E_{50} / J (impact)	-	-	1.8(±0.2) [h]	4.3(±0.3) [h]	2.5 - 4.0 [i]
$\rho_{crystal}$(calc.) / (g cm^{-3})	1.731 [k]	1.703 [l]	2.939 [l]	2.584 [m]	4.763 [n]
M / (g mol^{-1})	173.02 [o]	209.04 [o]	454.18 [o]	177.59 [o]	291.24 [o]

[a] obtained by DSC, heating rate 3 K min^{-1}

[b] D. J. Whelan, R. J. Spear, R. W. Read, The thermal decomposition of some primary explosives as studied by differential scanning calorimetry, *Thermochim. Acta*, 1984, **80**, 149-163; DSC data, heating rate 5 K min^{-1}

[c] ΔH_{exo} / (kJ mol^{-1}) = [ΔH_{exo} / (kJ g^{-1})] x [M / (g mol^{-1})]

[d] Bowden, F. P.; Williams, H. T. Initiation and Propagation of Explosion in Azides and Fulminates, *Proc. R. Soc. Lon. Ser.-A*, 1951, **208**, 176-188

[e] ΔH_{exo} / (kJ g^{-1}) = [ΔH_{exo} / (kJ mol^{-1})] / [M / (g mol^{-1})]; R. Meyer, J. Köhler, A. Homburg, Explosives, 6th ed. Wiley-VCH, Weinheim, 2007, state 1.6 kJ g^{-1} for the heat of explosion

[f] these estimates are based on the average molar contribution of the nitrotetrazolato group derived from DSC enthalpies of decomposition of **3** and **4** and mixtures thereof, 292(±17) kJ mol^{-1}, ignoring all other enthalpic effects

[g] ΔH_{exo} / (kJ cm^{-1}) = [ΔH_{exo} / (kJ mol^{-1})] / [M / (g mol^{-1})] x [$\rho_{crystal}$ / (g cm^{-3})]

[h] values obtained from material as synthesised without further processing; apparatus used for testing **3** and **4** is different to those used for LA

[i] data taken from T. M. Klapötke, C. M. Sabate, Safe 5-nitrotetrazolate anion transfer reagents, *Dalton Trans.*, 2009, 1835-1841, using BAM method

[k] data taken from T. M. Klapötke, C. M. Sabate, J. M. Welch, Alkali metal 5-nitrotetrazolate salts: prospective replacements for service lead(ii) azide in explosive initiators, *Dalton Trans.* 2008, 6372-6380.

[l] this paper

[m] data taken from J. W. Fronabarger, M. D. Williams, W. B. Sanborn, J. G. Bragg, D. A. Parrish and M. Bichay, DBX-1 – A Lead Free Replacement for Lead Azide, *Propell. Explos. Pyrotech.*, 2011, **36**, 541-550

[n] using a = 6.63, b = 16.25, c = 11.31 Å, Z = 12 given in L. V. Azaroff, Structural Investigation of Lead Azide, *Z. Kristallog. – Cryst. Mater.*, 1956, **107**, 362-369 leads to V = 1219 Å^3 and ρ = 4.76 g cm^{-3}

[o] calculated with ChemDraw Professional Version 18.0.0.231 (4029).

Table S3. Factors contributing to the outcome of the reduction reaction.

Factor	**Olive-green (amorphous) Material**					**$Cu_3Cl(N_4CNO_2)_2$**			**$Cu_3Cl(NT)_2$ - Cu(NT)**		**$Cu(N_4CNO_2)$**		
Na(NT).4H_2O reagent used		x	x	x		x	x	x	x	x	x	x	x
Na(NT).2H_2O reagent used	x				x								
deionised water as reaction solvent	x	x	x	x	x	x		x		x	x	x	x
distilled deionised water as reaction solvent							x		x				
NaHAsc addition regime applied	x				x	x	x	x	x	x	x	x	x
NaHAsc addition regime not applied		x	x	x									
Reaction vessel and stir bar rinsed with purified water (and mechanically cleaned with cellulose paper in most cases)	x	x		x	x	x	x		x		x		
Reaction vessel cleaned with hot aq. HNO_3 and neutralised with purified water			x					x		x		x	x
not externally seeded (or previously vessel)	x	x	x			x	x	x	x		x		
seeded with $Cu_3Cl(N_4CNO_2)_2$				x						x			x
seeded with $Cu(N_4CNO_2)$					x							x	
addition of 1/3 equiv. $ZnCl_2$ or $NiCl_2$								x					

Table S4. Geometric parameters of strong hydrogen bonds for compound **2**.

	Donor---H....Acceptor	D–H	H...A	D...A	D-H...A
1	O(3)--H(3A)..O(4)	0.84(2)	1.97(2)	2.7987(18)	170(2)
2	O(3)--H(3B)..O(4)	0.86(3)	1.97(3)	2.8140(18)	169(4)
3	O(4)--H(4A)..N(2)(α)	0.87	2.03	2.803(3)	147
4	O(4)--H(4A)..N(3)(α)	0.87	2.16	3.026(3)	171'
5	O(4)--H(4B)..O(2)	0.84(3)	2.10(3)	2.906(7)	161(2)
6	O(4)--H(4B)..N(4)(β)	0.84(3)	2.22(3)	2.976(9)	150(2)'

equivalent position codes: 4, 1-x,-y,1-z; 1, 3/2-x,1/2+y,3/2-z; 5, 1-x,1+y,3/2-z; 6, x,1-y,1/2+z.